CSMSA: Cross-Space Multiscale Adaptive Link Prediction for ceRNA-Mediated Multimolecular Disease Regulatory Networks

Junqi Long
School of Computer Science
Beijing University of Technology
Beijing, China
Junqilong@163.com

Jianqiang Li
School of Computer Science
Beijing University of Technology
Beijing, China
lijianqiang@bjut.edu.cn

Guangzhi Qu
Department of Computer Science and Engineering, Oakland University
Rochester, USA
gqu@oakland.edu

Kun Liu
School of Artificial Intelligence and Data Science
Hebei University of Technology
Tianjin, China
liukun@hebut.edu.cn

Bo Liu*
School of Mathematical and Computational Sciences
Massey University
Auckland, New Zealand
b.liu@massey.ac.nz

Abstract

Regulatory interactions associated with diseases are pivotal for elucidating the molecular mechanisms that drive disease progression and promoting precision medicine. Nevertheless, existing research algorithms often overlook the potential dynamic synergistic-competitive mechanisms between different ceRNA regulatory networks and lack cross-space learning capabilities across multiple heterogeneous graph structures, making it difficult to comprehensively capture the multidimensional molecular regulatory biological mechanisms in disease data with different structural densities. Therefore, we propose the cross-space multiscale adaptive learning framework (CSMSA) that integrates a heterogeneous five-layer ceRNA regulatory network and introduces an adaptive cross-space learning mechanism to dynamically capture complementary and specific interactions and effectively learn the intrinsic biological regulatory mechanisms. Moreover, the CSMSA framework employs a multi-scale feature fusion strategy that hierarchically learns node embeddings by integrating local structural information and global topological features from heterogeneous graphs to enhance predictive performance and robustness across complex datasets of varying sizes. Comprehensive evaluations on three independent datasets show that CSMSA surpasses existing methods in the multimolecular disease prediction task (Max AUC = 0.9880, Max AUPR = 0.9829), thereby providing a reliable new paradigm for probing disease regulatory links.

CCS Concepts

• **Applied computing** → **Bioinformatics**; **Biological networks**; **Computational genomics**; • **Computing methodologies** → **Knowledge representation and reasoning**; **Machine learning approaches**.

*Corresponding author.

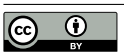

BCB '25, Philadelphia, PA, USA

ACM ISBN 979-8-4007-2200-4/2025/10
https://doi.org/10.1145/3765612.3767212

Keywords

Cross-space learning; Multi-scale fusion; ceRNA networks; Link prediction

ACM Reference Format:

Junqi Long, Jianqiang Li, Guangzhi Qu, Kun Liu, and Bo Liu. 2025. CSMSA: Cross-Space Multiscale Adaptive Link Prediction for ceRNA-Mediated Multimolecular Disease Regulatory Networks. In *Proceedings of the 16th ACM International Conference on Bioinformatics, Computational Biology, and Health Informatics (BCB '25), October 11–15, 2025, Philadelphia, PA, USA.* ACM, New York, NY, USA, 6 pages. https://doi.org/10.1145/3765612.3767212

1 Introduction

Competing endogenous RNAs (ceRNAs) embody a wide range of molecular regulatory relationships that play a critical role in disease expression mechanisms [1, 2]. In such networks, microRNAs (miRNAs) can function as decoys by binding to multiple RNA transcripts, while RNA molecules can act as ceRNAs by competitively binding to shared miRNAs, thereby collaboratively regulating disease initiation and progression [3–5]. This interplay gives rise to intricate and multilayered regulatory networks. Consequently, accurate prediction of regulatory relationships within disease-associated ceRNA networks offers a novel perspective for disease diagnosis and treatment. However, due to the inherent heterogeneity of data sources and the structural complexity of regulatory interactions, ceRNA-based disease link prediction remains a significant challenge in current biomedical research.

Early studies primarily relied on co-expression analysis or gene function annotation [6, 7] to estimate interactions between gene molecular. However, the resulting molecular interaction pairs were typically inferred at a superficial level based on expression similarity or functional description, lacking deeper insights into the underlying mechanisms of molecular interactions. Recently, with the advancement of graph neural networks (GNNs), researchers have increasingly studied the integration of molecular regulatory networks with graph-based models. In such frameworks, molecules are treated as graph nodes and their interactions as edges. Thus, the ceRNA regulatory link prediction task is reformulated as a multi-task relational prediction problem over heterogeneous molecular interaction graphs, enabling the effective learning of complex

molecular representations. For instance, VGAELDA [8] in lncRNA-disease link prediction task employs a graph autoencoder and variational inference to obtain efficient low-dimensional embeddings of lncRNA nodes. In multi-link prediction tasks among lncRNAs, miRNAs and diseases, the GCLMTP [9] and MGATE [10] models have achieved promising performance. These models respectively used graph autoencoders and graph contrastive learning frameworks to transform multi-link prediction tasks into multi-molecular feature learning, thereby effectively learning the representation of multi-type nodes.

However, existing models typically rely on static structural encodings, making it difficult to dynamically capture the synergy and specificity across multilayered ceRNA regulatory networks. And they are highly sensitive to structural density bias and imbalanced node distributions across different regulatory networks, which hampers the effective learning of unified node representations for multi-link prediction tasks. To address these limitations, we propose a Cross-space multiscale adaptive learning framework (CSMSA) for accurate multi-task prediction of disease-associated regulatory links based on competitive regulatory mechanisms of ceRNA interactions. In summary, the main contributions of our model are as follows:

- Constructed a heterogeneous five-layer ceRNA graph that incorporates inter-layer and intra-layer edges among lncRNAs, circRNAs, miRNAs, mRNAs, and diseases, thereby providing a unified view of regulatory associations across molecular layers.
- Proposed a graph-embedding learning framework based on a cross-space adaptive mechanism, enabling the dynamic capture of synergistic and specific representations among molecules within the ceRNA regulatory network.
- Introduced a multiscale dynamic feature-fusion strategy that optimally integrates local and global node information, thereby improving predictive performance and robustness across datasets of varying scales.
- Extracted unified node embeddings suited to multi-task prediction of disease-regulatory links and validated their effectiveness with multiple classifiers.

2 Related Work

Machine Learning-Based Link Prediction. Early traditional link prediction models predominantly relied on node-level feature extraction methods such as Singular Value Decomposition (SVD) [11] and Laplacian Eigenmaps (LE) [12] to capture structural patterns from biological networks, while employing traditional classifiers to infer similarities between node pairs. These methods depend heavily on manual feature extraction and are suitable for small-sample learning tasks, yet they fail to effectively capture the structural information of complex network.

Graph Autoencoder-Based Link Prediction. Autoencoder architectures have been widely applied in multi-molecular network modeling. Representative models such as GAERF [13], VGAELDA [8], LDNFSGB [14], and VAEMDA [15] typically adopt graph autoencoders (GAE) or variational graph autoencoders (VGAE) to extract node embedding representations. These methods exhibit advantages in handling data sparsity, but they still face challenges in learning structural-semantic consistency and capturing regulatory-specific.

Graph Contrastive Learning-Based Link Prediction. Contrastive learning has been introduced into the domain of graph representation learning in recent years. For example, its representative model representative model GCLMTP [9] constructs positive and negative sample pairs by perturbing the original graph structure and introduces an unsupervised contrastive objective to learn discriminative embeddings, thereby enhancing the robustness to complex regulatory patterns. However, these approaches predominantly focus on overall structural consistency, lacking the capacity to identify the specific regulatory features, making it difficult to achieve precise regulation link prediction in multi-space.

Graph Attention Mechanism-Based Link Prediction. Attention mechanisms have also been recently into disease link prediction tasks. For example, MGATE [10] incorporates intra-graph and inter-graph attention modules within a heterogeneous graph architecture to enhance node representation information. Nonetheless, most existing attention-based methods are limited to single-space graph encoding and lack the ability to dynamically fuse multi-space information, which constrains their generalizability in multi-source regulatory networks.

3 Method

3.1 Experimental datasets

In this study, we propose a unified feature learning framework for multi-space molecular regulatory link prediction, enabling effective feature extraction for lncRNA, circRNA, miRNA, mRNA, and disease nodes within complex ceRNA regulatory networks[1] (Fig. 1A). To rigorously assess its effectiveness and generalizability, we benchmark CSMSA on three independent public datasets.

Dataset 1 is derived from the LncACTdb v3.0 database, comprising 3,006 nodes and 15,217 experimentally validated molecular interaction edges. Dataset 2 is constructed by integrating data from multiple sources, including LncRNA2Target v2.0, Circ2Disease, miRTarBase v10.0, and cirbank, resulting in a total of 3,164 nodes and 111,867 regulatory edges. Dataset 3 incorporates large-scale data from RNADisease v4.0 and NPInter v5.0, containing 4,739 nodes and 224,412 regulatory interactions, thereby representing a more complex ceRNA regulatory network.

3.2 Cross-space adaptive learning mechanisms

Motivated by the biological regulatory mechanisms underlying ceRNA interactions, we propose a cross-space adaptive graph learning method that effectively captures unified node embedding representations across multi-type regulatory networks. The core idea of CSMSA mechanisms in constructing both Specific Attention and Common Attention modules for the ceRNA network (Fig. 1B) to achieve dynamic adaptive learning of the specific and synergistic expression relationships in the multi-molecular regulatory network driven by lncRNA and circRNA.

To capture the competitive regulatory relationships between the two molecular regulatory spaces, we define two independent

[1]All resources for this work are available at https://github.com/JunqiLab/CSMSA.

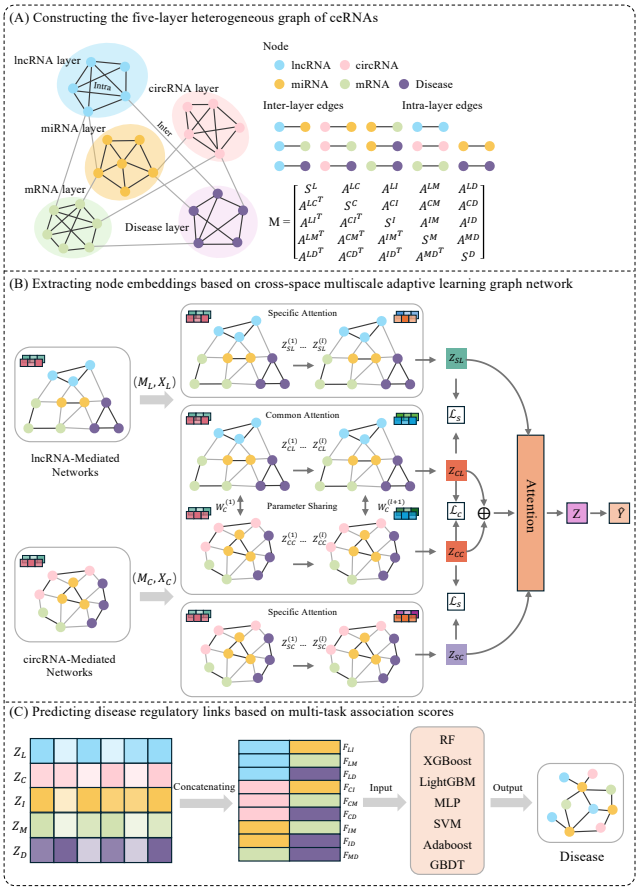

Figure 1: Overall framework for multimolecular disease link prediction. (A) Construction of a five-layer heterogeneous regulatory graph based on ceRNA molecules similarity and correlation. (B) Extraction of unified node embeddings. (C) Prediction of disease-associated regulatory links using the optimized multimolecular classifier.

Specific Attention modules to learn space-specific embeddings, denoted as Z_{SL} and Z_{SC}, and introduce a specificity constraint $\mathcal{L}_S$ to maintain the independence of these two regulatory spaces. Similarly, to efficiently learn the synergy between the two regulatory spaces, we define a shared-parameter Common Attention module to obtain the common embeddings Z_{CL} and Z_{CC}, and introduce a consistency constraint $\mathcal{L}_C$ to enhance their co-expression capacity.

Finally, the three space embedding vectors Z_{SL}, Z_{SC} and Z_C (the average of Z_{CL} and Z_{CC}) are adaptively dynamic fused using an attention mechanism to generate the final embedding Z, which is evaluated for its link discriminative ability by the inner calculation. Specifically, the attention weights α_{SL}, α_{SC} and α_C for each embedding space $s \in \{SL, SC, C\}$ are computed as defined in Eq. (1), and the final unified embedding Z is obtained through weighted dynamic fusion according to Eq. (2), where W is the learnable weight matrix that projects embeddings into the attention space, b is the bias vector, and q is the shared attention query vector that generates the attention scores for different embedding spaces.

$$\alpha_s = \frac{\exp\left(q^\top \cdot \tanh(W \cdot Z_s + b)\right)}{\sum_{s' \in S} \exp\left(q^\top \cdot \tanh(W \cdot Z_{s'} + b)\right)} \tag{1}$$

$$Z = \alpha_{SL} \cdot Z_{SL} + \alpha_{SC} \cdot Z_{SC} + \alpha_C \cdot Z_C \tag{2}$$

3.3 Multi-scale feature fusion strategy

To mitigate the alleviate the structural density bias and imbalanced node distribution across different regulatory networks, the Specific Attention and Common Attention modules further introduce a dynamic multiscale feature attention fusion strategy (Fig. 2).

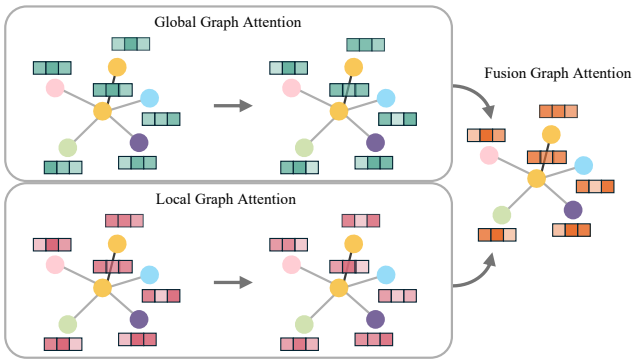

Figure 2: The multiscale dynamic feature fusion strategy: global graph attention, local graph attention, and fusion graph attention module.

This strategy employs a two-layer graph attention mechanism [16] to hierarchically extract and fuse the potential complementary information from both local structural features h_j^{loc} and global topological expression h_j^{glob}, thereby improving the discriminability of node embeddings, enhancing the robustness and accuracy across datasets of varying scales, with the $\ell + 1$ layer output denoted as Eq. (3), where σ is a nonlinear activation function, $\alpha_{ij}^{(l)}$ denotes the attention coefficient that measures the contribution of neighbor j to node i, $W^{(l)}$ is the learnable weight matrix that linearly projects the concatenated local and global features, and ω_1 and ω_2 are learnable scalar coefficients controlling the relative importance of $h_j^{(l,glob)}$ and $h_j^{(l,loc)}$ before linear transformation. The global features molecular regulatory relationship of this strategy are captured through the node2vec algorithm[17].

$$h_i^{(l+1)} = \sigma\left(\sum_{j \in \mathcal{N}} \alpha_{ij}^{(l)} \cdot W^{(l)} \left(\omega_1 \cdot h_j^{(l,glob)} \parallel \omega_2 \cdot h_j^{(l,loc)}\right)\right) \tag{3}$$

3.4 Objective Function

To effectively learn regulatory specificity within each Specific Attention space, we introduce the Hilbert-Schmidt Independence Criterion (HSIC) [18] and design a specificity constraint $\mathcal{L}_S$ to quantify the discrepancy between the embeddings of the lncRNA-specific space (Z_{CL}, Z_{SL}) and the circRNA-specific space (Z_{CC}, Z_{SC}). The HSIC loss is computed as:

$$\mathrm{HSIC}(Z_c, Z_s) = (n-1)^{-2} \cdot \mathrm{tr}(RK_cRK_s) \tag{4}$$

Where K_C and K_S are Gram matrices defined as $K(i,j) = Zi, Zj$ and $R = I - \frac{1}{n}ee^T$ is the centering matrix with identity matrix I and e is the all-one column vector. The loss is then given by:

$$\mathcal{L}_S = \mathrm{HSIC}(Z_{CL}, Z_{SL}) + \mathrm{HSIC}(Z_{CC}, Z_{SC}) \tag{5}$$

Although a shared parameter matrix is used across both Common Attention modules, we further impose a consistency constraint $\mathcal{L}_C$ to enhance the co-expression ability of the unified embeddings. This constraint is computed by comparing the normalized embeddings from the two Common Attention modules as:

$$\mathcal{L}_C = \left\| Z_{CL} \cdot Z_{CL}^\top - Z_{CC} \cdot Z_{CC}^\top \right\|_2^2 \tag{6}$$

Additionally, we compute the inner product between node embeddings z_i and z_j for each node pair (i, j) from the final embedding matrix $Z \in \mathbb{R}^{nxd}$ to estimate the link probability, as defined in Eq. (7), and the corresponding objective function is given in Eq. (8).

$$\hat{Y}_{ij} = \sigma\left(\mathbf{z}_i^\top \cdot \mathbf{z}_j\right) \tag{7}$$

$$\mathcal{L}_Y = -\sum_{(i,j)\in\mathcal{N}} \left[y_{ij} \log \hat{Y}_{ij} + (1 - y_{ij}) \log(1 - \hat{Y}_{ij}) \right] \tag{8}$$

Finally, the overall optimization objective combines all three loss is defined as Eq. (9), where γ and β are hyperparameters that control the strength of the consistency and specificity constraints, respectively.

$$\mathcal{L} = \mathcal{L}_Y + \gamma\mathcal{L}_C + \beta\mathcal{L}_S \tag{9}$$

3.5 Multimolecular link prediction

To achieve accurate multimolecular regulatory link prediction, we perform unified downstream multi-task training over all node pairs $(u, v) \in F$ using the embedding representations of the five node types $Z_l, Z_c, Z_i, Z_m, Z_d \subset Z$ (Fig. 1C). In this study, we systematically evaluate the link prediction performance of seven classifiers across different datasets, including Adaptive Boosting (Adaboost), Extreme Gradient Boosting (XGBoost), Gradient Boosted Decision Trees (GBDT), Light Gradient Boosting Machine (LightGBM), Multilayer Perceptron (MLP), Random Forest (RF), and Support Vector Machine (SVM).

4 Experiments Results

4.1 Ablation Study

To validate the effectiveness of the multiscale feature dynamic fusion module in the CSMSA framework, we conducted ablation experiments on datasets of varying scales and compared the embedding learning performance with and without this module (Table. 1). The results demonstrate that incorporating this module can significantly improve the link prediction performance of model across all datasets. Notably, a more substantial performance gain is observed on the small-scale Dataset 1, which contains fewer labeled samples. These findings indicate that the module can effectively captures the local structural information and global topological features across different nodes types through dynamic fusion strategy, thereby alleviating the problems of structural density deviation and imbalanced node distribution across different heterogeneous network, and enhancing the overall representational capacity of the model.

To further assess the effectiveness of the proposed cross-space adaptive learning mechanism, we compared the link prediction performance of embeddings generated from each individual space (Table. 1). The results show that the embeddings generated through cross-space mechanism consistently achieved the best predictive performance across all datasets, outperforming those generated from any single space. Overall, the proposed mechanism can automatically identify and integrate discriminative features from different molecular regulatory spaces, which helps to generate more expressive and robust unified node embeddings for accurate multimolecule link prediction.

Table 1: Ablation verification for the CSMSA.

Dataset	Scale Type	Multiscale		Space Type	Multispace	
		AUC	AUPR		AUC	AUPR
Dataset 1	Multi	**0.8826**	**0.8931**	All	**0.8826**	**0.8931**
	Single	0.8036	0.8439	Specific	0.8449	0.8296
				Common	0.8503	0.8505
Dataset 2	Multi	**0.8847**	**0.8490**	All	**0.8847**	**0.8490**
	Single	0.8534	0.8044	Specific	0.8780	0.8285
				Common	0.8628	0.8274
Dataset 3	Multi	**0.8876**	**0.8606**	All	**0.8876**	**0.8606**
	Single	0.8756	0.8058	Specific	0.8839	0.8181
				Common	0.8776	0.7842

4.2 Performance evaluation of the CSMSA unified embedding

Table 2: Performance comparison of classifiers and train ratios on three datasets.

Metric	Type	Dataset 1		Dataset 2		Dataset 3	
		AUC	AUPR	AUC	AUPR	AUC	AUPR
Down Stream	RF	**0.9637**	**0.9664**	**0.9831**	**0.9775**	**0.9880**	**0.9829**
	XGBoost	0.9460	0.9541	0.9716	0.9517	0.9827	0.9744
	LightGBM	0.9410	0.9455	0.9745	0.9663	0.9795	0.9731
	MLP	0.9472	0.9473	0.9739	0.9653	0.9792	0.9723
	SVM	0.9465	0.9463	0.9557	0.9191	0.9653	0.9462
	Adaboost	0.8721	0.8916	0.9493	0.9376	0.9659	0.9564
	GBDT	0.9156	0.9229	0.9685	0.9605	0.9757	0.9685
Train Ratio	80%	**0.9637**	**0.9664**	**0.9831**	**0.9775**	**0.9880**	**0.9829**
	60%	0.9387	0.9476	0.9797	0.9726	0.9847	0.9726
	40%	0.9014	0.9176	0.9772	0.9693	0.9816	0.9693

We evaluated the performance of the CSMSA unified embedding on three external datasets for multi-molecule prediction tasks. The results show (Table. 2) that RF performed best on all datasets(dataset

1: AUC = 0.9637, AUPR = 0.9664; dataset 2: AUC = 0.9831, AUPR = 0.9775; dataset 3: AUC = 0.9880, AUPR = 0.9829). In addition, we also conducted robustness tests in different training scales, and the results showed (Table. 2) that CSMSA maintained stable performance on datasets 2 and 3, and only slightly decreased on dataset 1 (AUC > 0.9014, AUPR > 0.9176). This effectively confirmed the feature representation and generalization capabilities of CSMSA unified embedding.

4.3 Performance comparison with other methods

To assess the advantage of CSMSA in multi-molecule ceRNA regulatory link prediction task, we compared it with seven representative baseline models across three datasets (Table. 3 and Table. 4). The results showed that CSMSA consistently outperformed all baseline models and had lower computational complexity. In contrast, CSMSA can jointly learn the synergy and specificity of multi-space molecular regulation through cross-space adaptive learning and multi-scale feature dynamic fusion strategy. However, SVD emphasizes global low-rank reconstruction while LE focuses on preserving local neighborhoods, both lacking adaptability to heterogeneous multi-space regulatory modeling. Although GAERF [13], VGAELDA [8] and ARGA [19] emphasize structural consistency or topological feature fusion, MGATE [10] and GCLMTP [9] introduce attention mechanism or contrastive learning to improve representation ability, they are all limited to the learning framework of a single space, and it is difficult to capture cross-space regulatory specificity.

Table 3: Performance comparison with baseline model.

Methods	Dataset 1		Dataset 2		Dataset 3	
	AUC	AUPR	AUC	AUPR	AUC	AUPR
CSMSA	**0.9637**	**0.9664**	**0.9831**	**0.9775**	**0.9880**	**0.9829**
GCLMTP	0.9253	0.8833	0.9447	0.9079	0.9566	0.9573
MGATE	0.8984	0.8481	0.9397	0.8996	0.9470	0.9082
GAERF	0.9551	0.9229	0.9165	0.8720	0.8904	0.8341
VGAELDA	0.8058	0.8494	0.8639	0.8530	0.8986	0.8794
ARGA	0.8245	0.8561	0.8576	0.8408	0.8962	0.8733
SVD	0.9477	0.8722	0.9079	0.7952	0.8683	0.7197
LE	0.9481	0.8726	0.9088	0.7974	0.8704	0.7226

Table 4: Complexity comparison with baseline models.

Model	Computational Complexity	Time (s)
CSMSA	$O(4 \cdot L \cdot (\|V\| \cdot d^2 + \|E\| \cdot d) + \|V\| \cdot d)$	0.1726
GCLMTP	$O(2 \cdot L \cdot (\|V\| \cdot d^2 + \|E\| \cdot d) + \|V\| \cdot d)$	0.1690
MGATE	$O(6 \cdot L \cdot (\|V\| \cdot d^2 + \|E\| \cdot d) + \|V\| \cdot d)$	0.9171
GAERF	$O(L \cdot (\|V\| \cdot d^2 + \|E\| \cdot d))$	0.1634
VGAELDA	$O(4 \cdot L \cdot (\|V\| \cdot d^2 + \|E\| \cdot d))$	0.1542
ARGA	$O(L \cdot (\|V\| \cdot d^2 + \|E\| \cdot d))$	0.1521
LE	$O(\|V\| \cdot k^2 + \|E\| \cdot k)$	0.1511
SVD	$O(\|V\|^3)$	7.0850

4.4 Case Study

To further validate the reliability of the CSMSA framework, we conducted a case study on breast cancer (DOID: 1612), which has the highest incidence rate among women worldwide [20] in three independent datasets. The primary objective was to identify potential regulatory interactions among lncRNAs, circRNAs, miRNAs, and mRNAs associated with the disease. We predicted the molecular regulatory links of the top ten multi-omics candidate genes (Fig 3). The results showed that all predicted genes were verified in relevant public databases, and the inferred regulatory network was mediated by 10 lncRNAs and 5 circRNAs, which acted together in mir-148 [21] and mir-200 [22] to regulate the expression of IGF1R [23], ITGB1 [24], VEGFA [25] and FOXO3 [26] in cancer immunity, oncogenic signaling, cell cycle and DNA repair pathway [27]. Notably, the framework also correctly identified circRNA-specific regulatory links involving NOTCH2 [28] and SOCS1 [29]. These results highlight CSMSA's strong capability to capture both synergistic and specific regulatory patterns within complex multi-space ceRNA networks, demonstrating its effectiveness and interpretability in multi-molecular disease link prediction task.

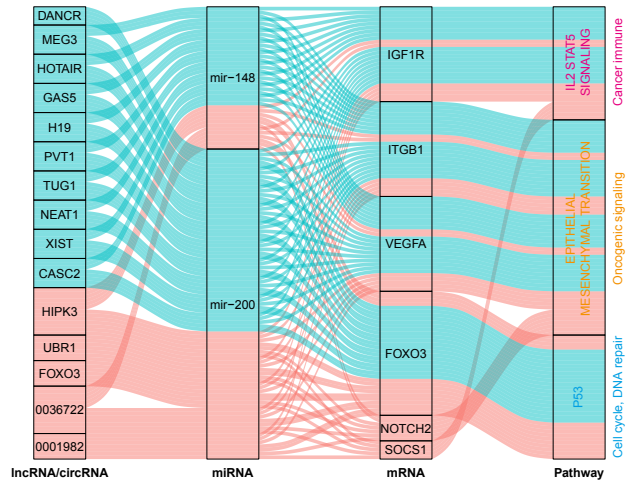

Figure 3: Regulatory links predicted for the top 10 candidate genes associated with breast cancer.

5 Conclusion

We proposed a unified modeling framework CSMSA for multi-molecule ceRNA regulatory network link prediction tasks. Through cross-space adaptive learning mechanism and multi-scale feature fusion strategy, dynamic attention learning is performed on specific space and common space features driven by lncRNA and circRNA to effectively learn the complementarity and specificity between different regulatory networks. Many experimental results show that CSMSA exhibits optimal performance and generalization ability in multi-task regulatory link prediction, especially in the face of small samples and complex networks with strong structural heterogeneity.

In addition, we further evaluated the practical deployment capabilities of the CSMSA framework. The total computational complexity is $O(4 \cdot L \cdot (|V| \cdot d^2 + |E| \cdot d) + |V| \cdot d)$, with an average training time of approximately 0.17 seconds per epoch on the largest dataset (Dataset 3). In practical scenarios, since biological regulatory networks are typically sparse graphs ($|E| \ll |V|^2$) and the feature dimension d is relatively small, the model framework demonstrates strong scalability and computational efficiency. Therefore, it is well-suited for large-scale biological network analysis predictions tasks.

Although CSMSA demonstrates strong performance in multi-space molecular regulatory link prediction, several limitations remain. The current framework relies heavily on existing molecular interactions, which may reduce its adaptability to emerging molecular types. Furthermore, the model has not yet incorporate temporal dynamics or tissue-specific expression patterns, which may limit its applicability in modeling time-dependent disease progression. Future work can further enhance the biological interpretability and clinical applicability of the model by expanding more complex pathological regulatory space structures and introducing patient genetic phenotypic characteristics, providing more precise and comprehensive insights into disease mechanisms and therapeutic strategies.

Acknowledgments

We thank the anonymous reviewers for their valuable comments. This study was partially supported by National Natural Science Foundation of China (Grant Number: 62076015) and the REaDI Fund of Massey University.

References

[1] Maryam Kohansal, Yasemin Khudiar Alghanimi, Shaimaa R Banoon, Abdolmajid Ghasemian, Hamed Afkhami, Abdolreza Daraei, Zhangling Wang, Najmeh Nekouian, Jindong Xie, and Xinpei Deng. 2024. CircRNA-associated ceRNA regulatory networks as emerging mechanisms governing the development and biophysiopathology of epilepsy. *CNS Neuroscience & Therapeutics* 30, 4 (2024), e14735. doi:10.1111/cns.14735

[2] Jianhao Jiang, Ilgiz Gareev, Tatiana Ilyasova, Alina Shumadalova, Weijie Du, and Baofeng Yang. 2024. The role of lncRNA-mediated ceRNA regulatory networks in liver fibrosis. *Non-coding RNA research* 9, 2 (2024), 463–470. doi:10.1016/j.ncrna.2024.01.001

[3] Deepshikha Singh, Yehuda G. Assaraf, and Rajesh N. Gacche. 2022. Long non-coding RNA mediated drug resistance in breast cancer. *Drug Resist Updat* 63 (2022), 100851. doi:10.1016/j.drup.2022.100851

[4] Jichuan Xu, Jian Xu, Xinyuan Liu, and Jianxin Jiang. 2022. The role of lncRNA-mediated ceRNA regulatory networks in pancreatic cancer. *Cell Death Discov* 8, 1 (2022), 287. doi:10.1038/s41420-022-01061-x

[5] Yunpeng Zhang, Yanjun Xu, Li Feng, Feng Li, Zeguo Sun, Tan Wu, Xinrui Shi, Jing Li, and Xia Li. 2016. Comprehensive characterization of lncRNA-mRNA related ceRNA network across 12 major cancers. *Oncotarget* 7, 39 (2016), 64148–64167. doi:10.18632/oncotarget.11637

[6] Paola Paci, Giulia Fiscon, Federica Conte, Rui-Sheng Wang, Lorenzo Farina, and Joseph Loscalzo. 2021. Gene co-expression in the interactome: moving from correlation toward causation via an integrated approach to disease module discovery. *npj Systems Biology and Applications* 7, 1 (2021), 3. doi:10.1038/s41540-020-00168-0

[7] Sipko van Dam, Urmo Võsa, Adriaan van der Graaf, Lude Franke, and João Pedro de Magalhães. 2017. Gene co-expression analysis for functional classification and gene–disease predictions. *Briefings in Bioinformatics* 19, 4 (2017), 575–592. doi:10.1093/bib/bbw139

[8] Zhuangwei Shi, Han Zhang, Chen Jin, Xiongwen Quan, and Yanbin Yin. 2021. A representation learning model based on variational inference and graph autoencoder for predicting lncRNA-disease associations. *BMC Bioinformatics* 22, 1 (2021), 136. doi:10.1186/s12859-021-04073-z

[9] Nan Sheng, Yan Wang, Lan Huang, Ling Gao, Yangkun Cao, Xuping Xie, and Yuan Fu. 2023. Multi-task prediction-based graph contrastive learning for inferring the relationship among lncRNAs, miRNAs and diseases. *Briefings in Bioinformatics* 24, 5 (2023), bbad276. doi:10.1093/bib/bbad276

[10] Nan Sheng, Lan Huang, Yan Wang, Jing Zhao, Ping Xuan, Ling Gao, and Yangkun Cao. 2022. Multi-channel graph attention autoencoders for disease-related lncRNAs prediction. *Briefings in Bioinformatics* 23, 2 (2022), bbab604. doi:10.1093/bib/bbab604

[11] Huilin Tan, Zhen Zhang, Xin Liu, Yiming Chen, Zinuo Yang, and Lei Wang. 2024. MDSVDNV: predicting microbe–drug associations by singular value decomposition and Node2vec. *Frontiers in Microbiology* 14 (2024). doi:10.3389/fmicb.2023.1303585

[12] Yulian Ding, Xiujuan Lei, Bo Liao, and Fang-Xiang Wu. 2022. MLRDFM: a multi-view Laplacian regularized DeepFM model for predicting miRNA-disease associations. *Briefings in Bioinformatics* 23, 3 (03 2022), bbac079. doi:10.1093/bib/bbac079

[13] Qing-Wen Wu, Jun-Feng Xia, Jian-Cheng Ni, and Chun-Hou Zheng. 2021. GAERF: predicting lncRNA-disease associations by graph auto-encoder and random forest. *Briefings in Bioinformatics* 22, 5 (2021), bbaa391. doi:10.1093/bib/bbaa391

[14] Yuan Zhang, Fei Ye, Dapeng Xiong, and Xieping Gao. 2020. LDNFSGB: prediction of long non-coding rna and disease association using network feature similarity and gradient boosting. *BMC Bioinformatics* 21, 1 (2020), 377. doi:10.1186/s12859-020-03721-0

[15] Li Zhang, Xing Chen, and Jun Yin. 2019. Prediction of potential miRNA–disease associations through a novel unsupervised deep learning framework with variational autoencoder. *Cells* 8, 9 (2019), 1040. doi:10.3390/cells8091040

[16] Petar Velickovic, Guillem Cucurull, Arantxa Casanova, Adriana Romero, Pietro Lio, and Yoshua Bengio. 2017. Graph attention networks. *stat* 1050, 20 (2017), 10–48550. doi:10.48550/arXiv.1710.10903

[17] Aditya Grover and Jure Leskovec. 2016. node2vec: Scalable Feature Learning for Networks. https://api.semanticscholar.org/CorpusID:207238980

[18] Le Song, Alex Smola, Arthur Gretton, Karsten M. Borgwardt, and Justin Bedo. 2007. Supervised feature selection via dependence estimation. 823–830 pages. doi:10.1145/1273496.1273600

[19] Shirui Pan, Ruiqi Hu, Guodong Long, Jing Jiang, Lina Yao, and Chengqi Zhang. 2018. Adversarially regularized graph autoencoder for graph embedding. 2609–2615 pages. doi:10.48550/arXiv.1802.04407

[20] Rebecca L. Siegel, Angela N. Giaquinto, and Ahmedin Jemal. 2024. Cancer statistics, 2024. *CA Cancer J Clin* 74, 1 (2024), 12–49. doi:10.3322/caac.21820

[21] J. Xu, L. Lin, Q. Chen, and L. Li. 2023. Hsa-miR-148a-3p promotes malignant behavior of breast cancer cells by downregulating DUSP1. *Nan Fang Yi Ke Da Xue Xue Bao* 43, 9 (2023), 1515–1524. doi:10.12122/j.issn.1673-4254.2023.09.09

[22] Minh TN Le, Peter Hamar, Changying Guo, Emre Basar, Ricardo Perdigão-Henriques, Leonora Balaj, and Judy Lieberman. 2014. miR-200–containing extracellular vesicles promote breast cancer cell metastasis. *The Journal of clinical investigation* 124, 12 (2014), 5109–5128. doi:10.1172/jci75695

[23] Qing Xu, Yue Jiang, Yu Yin, Qi Li, Jun He, Yi Jing, Yan-Ting Qi, Qian Xu, Wei Li, Bo Lu, Stephen S. Peiper, Bing-Hua Jiang, and Ling-Zhi Liu. 2013. A regulatory circuit of miR-148a/152 and DNMT1 in modulating cell transformation and tumor angiogenesis through IGF-IR and IRS1. *J Mol Cell Biol* 5, 1 (2013), 3–13. doi:10.1093/jmcb/mjs049

[24] Sukhontip Klahan, Wan-Chen Huang, Che-Mai Chang, Henry Sung-Ching Wong, Chi-Cheng Huang, Mei-Shin Wu, Yu-Chiao Lin, Hsing-Fang Lu, Ming-Feng Hou, and Wei-Chiao Chang. 2016. Gene expression profiling combined with functional analysis identify integrin beta1 (ITGB1) as a potential prognosis biomarker in triple negative breast cancer. *Pharmacological research* 104 (2016), 31–37. doi:10.1016/j.phrs.2015.12.004

[25] Hsiang-Lin Tsai, Zhi-Feng Miao, Yi-Ting Chen, Ching-Wen Huang, Yung-Sung Yeh, I-Ping Yang, and Jaw-Yuan Wang. 2019. miR-148a inhibits early relapsed colorectal cancers and the secretion of VEGF by indirectly targeting HIF-1α under non-hypoxia/hypoxia conditions. *J Cell Mol Med* 23, 5 (2019), 3572–3582. doi:10.1111/jcmm.14257

[26] Fayyaz Ahmed, Muhammad Adnan, Ayesha Malik, Somayya Tariq, Farukh Kamal, and Bushra Ijaz. 2021. Perception of breast cancer risk factors: Dysregulation of TGF-β/miRNA axis in Pakistani females. *Plos one* 16, 7 (2021), e0255243. doi:10.1371/journal.pone.0255243

[27] Aravind Subramanian, Pablo Tamayo, Vamsi K. Mootha, Sayan Mukherjee, Benjamin L. Ebert, Michael A. Gillette, Amanda Paulovich, Scott L. Pomeroy, Todd R. Golub, Eric S. Lander, , and Jill P. Mesirov. 2005. Gene set enrichment analysis: a knowledge-based approach for interpreting genome-wide expression profiles. *Proc Natl Acad Sci U S A* 102, 43 (2005), 15545–50. doi:10.1073/pnas.0506580102

[28] Yi-Ping Fu, Hege Edvardsen, Alpana Kaushiva, Juan P Arhancet, Tiffany M Howe, Indu Kohaar, Patricia Porter-Gill, Anushi Shah, Hege Landmark-Høyvik, and Sophie D Fosså. 2010. NOTCH2 in breast cancer: association of SNP rs11249433 with gene expression in ER-positive breast tumors without TP53 mutations. *Molecular cancer* 9 (2010), 1–11. doi:10.1186/1476-4598-9-113

[29] MK Evans, CR Yu, A Lohani, RM Mahdi, X Liu, AR Trzeciak, and CE Egwuagu. 2007. Expression of SOCS1 and SOCS3 genes is differentially regulated in breast cancer cells in response to proinflammatory cytokine and growth factor signals. *Oncogene* 26, 13 (2007), 1941–1948. doi:10.1038/sj.onc.1209993